Received 22 October 2022; accepted 8 November 2022. Date of publication 16 November 2022; date of current version 23 November 2022.

Digital Object Identifier 10.1109/OJCOMS.2022.3222576

Reliability of Spectrum-Efficient Mixed Satellite-Underwater Systems

CHRISTINA GAMAL [1] (Student Member, IEEE), MOHAMED ELSAYED [1] (Student Member, IEEE), AHMED SAMIR [1] (Student Member, IEEE), HEBA A. TAGELDIEN [1], SYMEON CHATZINOTAS [2] (Senior Member, IEEE), MOSTAFA M. FOUDA [3] (Senior Member, IEEE), AND BASEM M. ELHALAWANY [1] (Senior Member, IEEE)

[1]Faculty of Engineering at Shoubra, Benha University, Cairo 11511, Egypt

[2]Interdisciplinary Centre for Security, Reliability and Trust, University of Luxembourg, 1855 Luxembourg City, Luxembourg

[3]Department of Electrical and Computer Engineering, Idaho State University, Pocatello, ID 83209, USA

CORRESPONDING AUTHOR: B. M. ELHALAWANY (e-mail: basem.mamdoh@feng.bu.edu.eg)

ABSTRACT The combination of radio-frequency (RF) communication and underwater optical wireless communication (UOWC) plays a vital role in the underwater Internet of Things (UIoT). This correspondence proposes a dual-hop hybrid satellite underwater system that exploits non-orthogonal multiple access (NOMA) as a spectrum-efficient access technique. The RF link from the satellite to the relay on an oil platform is presumptively subject to a Shadowed-Rician (SR) fading, while the UOWC channels from the relay to the underwater destinations are suggested to follow Exponential-Generalized Gamma (EGG) distributions. The reliability of the system is characterized in terms of both underwater destinations and system outage probabilities (OPs). We derive new closed-form expressions for the OPs under imperfect successive interference cancellation (SIC) conditions. Furthermore, the asymptotic OP and the diversity order (DO) are obtained to learn more about the system's performance. The results are verified through an extensive representative Monte-Carlo simulation. Also, we investigate the performance against the turbulence of the salty water, air bubbles level (BL), temperature gradients (TG), shadowing parameters, and satellite pointing errors due to satellite motion, even if the beam is pointed at the center of the directive antenna relay, the beam will randomly oscillate. Finally, we contrast our approach with the conventional orthogonal multiple access (OMA) scheme to demonstrate its superiority.

INDEX TERMS Satellite, underwater optical wireless communication, non-orthogonal multiple access, outage probability.

I. INTRODUCTION

THE RISE of underwater and satellite communication needs has drawn attention to the hybrid underwater-satellite networks, which have been noticed in many critical UIoT applications. Recently, an increase in interest in researching a variety of purposes for the underwater ecosystem, including climate change monitoring, marine animal research, observation of oil rigs, surveillance, scientific data collection underwater, marine and coastal pollution monitoring, and autonomous operations. Recently, underwater wireless communications (UWCs) have been implemented using blue/green optical wavelengths, due to their advantages such as higher data rates, bandwidth, and low latency compared with radio-frequency (RF) waves and acoustic waves. Contrary, underwater optical wireless communication (UOWC) suffers from turbulence, scattering, absorption, and limited power transmission [1], [2]. On the other side, the acoustic-based underwater communication suffers from some drawbacks include significant attenuation, low data rates, high bit error rates, low speed, low bandwidth, and excessive delay. Additionally, it is negatively impacted by the salt and turbulence of the water, which hinders its effectiveness in the water channel. On the other side, the features of the water channel do not affect RF waves but the electrical

conductivity of the water does. Additionally, RF is costly and only has very limited communication ranges [3]. In the literature, efforts have been devoted to characterizing the UOWC model systems and analyzing the performance. In [4], [5] the UOWC model has been proposed over mixed Exponential-Generalized Gamma (EGG), including the effect of turbulence for both fresh and saltwater, with temperature gradient and air bubbles.

In [6], authors investigated the effectiveness of multiple-input multiple-output (MIMO) UOWC systems using on-off keying (OOK) modulation in the presence of turbulence, absorption, and scattering of optical waves. Further, the UOWC can be linked to the terrestrial communication system via RF links with dual-hop cooperative protocols, which enables the underwater real-time monitoring systems. It has been indicated in [7] that the relaying node is necessary for extending the communication range for UOWC systems. In [5], [8], authors have studied the effectiveness of the amplify-and-forward (AF) relaying protocol with a dual-hop UWOC system.

Satellite networks provide wide coverage and rapid deployment of terrestrial wireless communication systems [9]. Hence, integrating underwater with satellite communications will further extend the applications of space-underwater integration. In [10], authors have proposed an asymmetric satellite-UOWC system based on a decode-and-forward (DF) relay for oceanic monitoring purposes, where the UWOC was based on cascaded independent non-identically distributed Gamma-Gamma channel coefficients and the satellite link was a Shadowed-Rician distribution. A hybrid satellite-underwater acoustic was presented in [11]. The authors in [12], have evaluated the average bit error rate's closed-form expression for a satellite-UOWC system that used EGG distribution for the UWOC link. The performance of a hybrid satellite-UWOC system's secrecy has been investigated in [13], where an Unmanned Aerial Vehicle (UAV) was considered as an eavesdropper for the satellite link.

Non-orthogonal multiple access (NOMA) has been investigated for improving the spectral efficiency of UOWC systems [14], [15], [16]. NOMA improves performance over the standard orthogonal multiple access (OMA) approaches by allowing several users to share the same frequency/time resource while exploiting the power domain by multiplexing the signals of several users at various power levels [17], [18], [19], [20], [21], [22]. As a result, users with better channel gains decode and exclude messages meant for other users before decoding their own messages using the successive interference cancellation (SIC) technique. However, practical SIC techniques are not perfect which may lead to error propagation and decoding errors [23]. Satellite communications are crucial for oil operations since oil activities frequently take place in the most remote areas where there is no terrestrial network infrastructure. Many works have studied merging satellites with oil platforms as monitoring oil pollution to ensure environmental safety to avoid the risk of spill accidents by using underwater sensors for monitoring any unusual actions and taking necessary precautions [24], [25]. So this motivated us to build a system connecting the satellite and underwater sensors through a relay placed on an oil platform for monitoring and data exchanging applications.

As far as the authors' knowledge goes, the research on hybrid satellite-UOWC based on the NOMA scheme with imperfect SIC is still not investigated. Inspired by the aforementioned observation, we propose a hybrid satellite-UOWC based on the NOMA scheme with imperfect SIC. The contribution of this paper is to (1) derive a new closed-form expression of OP assuming that the RF channel distribution undergoes Shadowed-Rician and the UOWC channel has EGG fading. (2) Obtain an asymptotic expression of the OP and hence the diversity order of the proposed system. (3) Verify our analysis via an extensive Monte-Carlo simulation while changing various parameters including shadowing conditions and different pointing error angles for the RF link, as well as temperature gradients and air bubbles at different water levels for the underwater link. (4) Finally, compare the proposed system with a benchmark OMA-based system.

This paper's remaining sections are organised as follows: in Section II, the suggested system and channel models are explained, while in Section III, analytical formulations of the exact and asymptotic OPs and the diversity order are produced. Illustrative numerical outcomes are shown in Section IV. The concluding statements are defined in Section V.

Notations: $(.)_n$ is the pochhammer symbol, $E[.]$ is the expectation, $|.|$ is the absolute value, $\Gamma(.)$ is the gamma function, and $G_{p,q}^{m,n}[.]$ is the Meijer-G function [26].

II. SYSTEM MODEL AND CHANNEL STATISTICS

A. SYSTEM MODEL

In this paper, we take into consideration a hybrid downlink satellite-UOWC based on the NOMA scheme with imperfect SIC. The system model consisting of a low earth orbit (LEO) Iridium satellite (S) with L-band, decode and forward (DF) Relay (R) on the surface of an oil platform, and two underwater destinations (D_i), $i \in \{f, n\}$, i.e., D_f and D_n are considered to be a far destination and a near destination, respectively, as shown in Fig. 1. We assume that under the half-duplex communication mode, each node has a single antenna. Thus, the satellite transmits data to the two destinations in two time slots. S transmits a superimposed signal $x_s = \sqrt{a_f p_s} x_f + \sqrt{a_n p_s} x_n$ over RF channel to DF R during the first time slot, where x_f and x_n are the signals for D_f and D_n, respectively, a_f and a_n are the NOMA power allocation factors for D_f and D_n at S, respectively, p_s is the total power transmitted at S.

The received signal y_R at R from S can be written as $y_R = h_s \sqrt{Q} x_s + n_s$ where h_s denotes the channel fading coefficient of the RF channel from S to R with gain expectation $\mathrm{E}[|h_s|^2] = 1$, the additive white Gaussian noise (AWGN) is represented by $n_s \sim \mathcal{CN}(0, \sigma_s^2)$, which has a variance

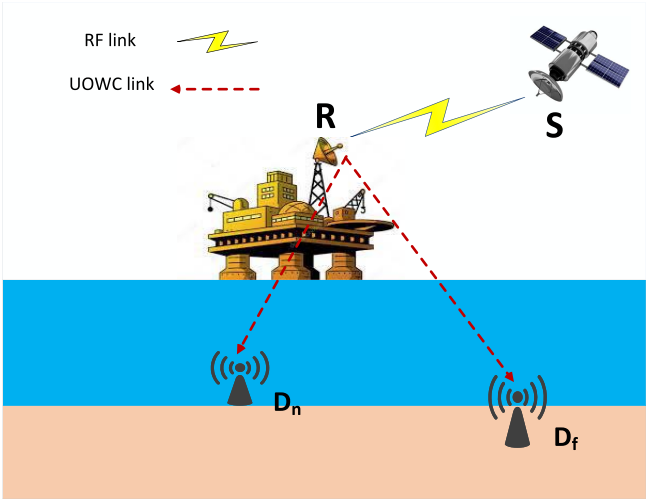

FIGURE 1. Block diagram of hybrid satellite/UOWC based on NOMA system.

of σ_s^2 and a mean of 0. Q represents the link budget from satellite to relay and can be given by $Q = \frac{G_s(\phi)G_R}{L_f L_p}$, where $G_s(\phi)$ is the beam gain and can be calculated as [27] $G_s(\phi) = G_s(\frac{J_1(u)}{2u} + 36\frac{J_3(u)}{u^3})^2$, $J_1(.)$ and $J_3(.)$ are the first-kind Bessel function with order one and three, respectively, $u = 2.07123\,\frac{d}{r}$, r denotes the radius of the beam, and the distance between the beam's boresight and the relay is denoted by d, G_s is the maximum antenna gain of the satellite, G_R is the receiver antenna gain, L_p and L_f represent the depointing loss and free-space loss, respectively. L_p can be formulated in dB as [28, (5.4b, 5.18)] $L_p = 2.7211 * 10^{-20} f_s^2 D_s^2 \theta_e^2$ where f_s, D_s, and θ_e denote downlink carrier frequency, antenna aperture diameter and pointing error angle at the satellite, respectively. $L_f = \frac{4\pi f_s h}{c}$, where h denotes the satellite's height and c denotes the light's velocity.

The relay first decodes x_f, assuming that the NOMA power allocation factors $a_f > a_n$ and $a_f + a_n = 1$, then uses SIC to decode x_n, based on NOMA method. Hence, the signal-to-interference-plus-noise ratios (SINRs) of decoding x_f and x_n at R can be respectively expressed as $\gamma_R^f = \frac{a_f \rho_s |h_s|^2 Q}{a_n \rho_s |h_s|^2 Q + 1}$, and $\gamma_R^n = \frac{a_n \rho_s |h_s|^2 Q}{\eta a_f \rho_s |h_s|^2 Q + 1}$ respectively assuming imperfect SIC conditions where $\rho_s = p_s/\sigma_s^2$ denotes the transmit signal-to-noise ratio (SNR) at S, and η denotes the residual interference signal cancellation factor ($0 \le \eta \le 1$).

In the second time slot, R decodes and retransmits a received superimposed signal $x_R = \sqrt{b_f p_R} x_f + \sqrt{b_n p_R} x_n$ over UOWC channels to the two destinations, where b_f and b_n are the NOMA power allocation factors for D_f and D_n at R, respectively, p_R is the total power transmitted at R. Hence, the received signals at the far and near destinations are respectively expressed as $y_{Df} = \varepsilon_f |h_f|^2 x_R + n_u$ and $y_{Dn} = \varepsilon_n |h_n|^2 x_R + n_u$, where n_u denotes AWGN with zero mean and variance σ_u^2, ε_f and ε_n represent photodetectors responsivity (i.e., $\varepsilon_f = \varepsilon_n \cong 1$), and h_f and h_n are the channel fading coefficients of UOWC with $E[|h_f|^2] = E[|h_n|^2] = 1$ for R-D_f and R-D_n links respectively. According to NOMA technique, D_f decodes the received signal to extract its own signal, as we assume that $b_f > b_n$ and $b_f + b_n = 1$. The SINR at D_f to decode x_f is $\gamma_{Df}^f = \frac{b_f \rho_R |h_f|^2}{b_n \rho_R |h_f|^2 + 1}$, while, D_n first decodes x_f then uses SIC to extract x_n. Consequently, the SINRs to decode x_f and x_n at D_n are respectively expressed as $\gamma_{Dn}^f = \frac{b_f \rho_R |h_n|^2}{b_n \rho_R |h_n|^2 + 1}$, and $\gamma_{Dn}^n = \frac{b_n \rho_R |h_n|^2}{\eta b_f \rho_R |h_n|^2 + 1}$, where $\rho_R = p_R/{\sigma_u}^2$ is the transmit SNR.

B. CHANNEL STATISTICS

The UOWC channels, h_i, between R and D_i are assumed to follow EGG distribution, in which the cumulative distribution function (CDF) is expressed as [4], [29]

$$F_{|h_i|^2}(x) = w\, G_{1,2}^{1,1}\left(\frac{1}{\lambda}\left(\frac{x}{\mu_r}\right)^{\frac{1}{r}}\middle| \begin{matrix} 1 \\ 1, 0 \end{matrix}\right) + \frac{1-w}{\Gamma(a)} G_{1,2}^{1,1}\left(\frac{1}{b^c}\left(\frac{x}{\mu_r}\right)^{\frac{c}{r}}\middle| \begin{matrix} 1 \\ a, 0 \end{matrix}\right), \quad (1)$$

where λ is the parameter for the exponential distribution, a, b, and c are the parameters used to characterize the generalized Gamma distribution, $0 < w < 1$ is the mixture coefficient between the two distributions, and the average electrical SNR is calculated based on the kind of receiver detection, such as heterodyne detection (r = 1) or intensity modulation/direct detection (IM/DD) (r = 2) such that

$$\mu_r = \begin{cases} \Omega_x & r = 1 \\ \frac{\Omega_x}{2w\lambda^2 + b^2(1-w)\Gamma\left(a+\frac{2}{c}\right)/\Gamma(a)} & r = 2, \end{cases} \quad (2)$$

where Ω_x is the average SNR of the UOWC links. On the other side, the RF channel, h_s, the link between S and R is assumed to experience Shadowed-Rician distribution, in which the CDF is given by [30]

$$F_{|h_s|^2}(x) = 1 - \alpha e^{-(\beta-\delta)x} \sum_{k=0}^{m-1} \psi(k) \sum_{l=0}^{k} \frac{k!}{l!} x^l (\beta - \delta)^{-(k-l+1)}, \quad (3)$$

where SR distribution's parameters are α, β, and δ, $\psi(k) = \frac{(-1)^k (1-m)_k \delta^k}{(k!)^2}$, and the severity parameter is m.

III. OUTAGE PROBABILITY ANALYSIS

Outage probability is considered as one of the important metrics to evaluate the performance of communication systems and to determine if the receiver can effectively decode its own information. So in this section, we evaluate the reliability of the proposed system in terms of OPs of both destinations nodes and the overall system. We also estimate the asymptotic OP and the diversity order.

A. OP OF D_F

The outage at the far destination happens when the R or the D_f fail to decode the signal x_f such that the received SINR falls below the target threshold value [31]. Hence the

outage probability of the far destination denoted by OP_f can be formulated as

$$\begin{aligned} OP_f &= 1 - \Pr\left(\gamma_R^f > \gamma_f, \gamma_{Df}^f > \gamma_f\right) \\ &= 1 - \Pr\left(|h_s|^2 > \frac{\tau_1}{\rho_s Q}\right) \times \Pr\left(|h_f|^2 > \frac{\nu_1}{\rho_R}\right), \end{aligned} \quad (4)$$

where $\gamma_f = 2^{R_f} - 1$ is the threshold SNR relating to the target data rate R_f at the D_f to detect x_f, $\tau_1 = \frac{\gamma_f}{a_f - a_n\gamma_f}$ with $a_f > a_n\gamma_f$, and $\nu_1 = \frac{\gamma_f}{b_f - b_n\gamma_f}$ with $b_f > b_n\gamma_f$. By using the CDFs in (1) and (3) and substituting in (4), the closed-form expression of OP_f can be obtained as (5), shown at the bottom of the page.

B. OP OF D_N

The outage at the near destination happens when the R or the D_n fail to decode the signal x_f or x_n, as detecting x_n at D_n needs first to detect x_f then use SIC to remove x_f based on NOMA. Hence the outage probability at near destination denoted by OP_n can be formulated as

$$\begin{aligned} OP_n &= 1 - \Pr\left(\gamma_R^f > \gamma_f, \gamma_R^n > \gamma_n, \gamma_{Dn}^f > \gamma_f, \gamma_{Dn}^n > \gamma_n\right) \\ &= 1 - \Pr\left(|h_s|^2 > \frac{\tau}{\rho_s Q}\right) \times \Pr\left(|h_n|^2 > \frac{\nu}{\rho_R}\right), \end{aligned} \quad (6)$$

where $\gamma_n = 2^{R_n} - 1$ is the threshold SNR relating to the target data rate R_n at the D_n to detect x_n, $\tau = \max(\tau_1, \tau_2)$, $\tau_2 = \frac{\gamma_n}{a_n - \eta a_f \gamma_n}$ with $a_n > \eta a_f \gamma_n$, $\nu = \max(\nu_1, \nu_2)$, and $\nu_2 = \frac{\gamma_n}{b_n - \eta b_f \gamma_n}$ with $b_n > \eta b_f \gamma_n$. By substituting (1) and (3) in (6), the closed-form expression of OP_n can be written as in (7), shown at the bottom of the page.

C. OP OF THE SYSTEM

The probability that one of the receiver nodes in the proposed system, or all of the receiver nodes, which are the relay, near and far destinations, experiences an outage denotes the system outage probability OP_{sys}, which can be written as

$$\begin{aligned} OP_{sys} &= 1 - \Pr\left(\gamma_R^f > \gamma_f, \gamma_R^n > \gamma_n, \gamma_{Df}^f > \gamma_f, \gamma_{Dn}^f > \gamma_f, \right. \\ &\qquad \left. \gamma_{Dn}^n > \gamma_n\right) \\ &= 1 - \Pr\left(|h_s|^2 > \frac{\tau}{\rho_s Q}\right) \times \Pr\left(|h_n|^2 > \frac{\nu}{\rho_R}\right) \\ &\quad \times \Pr\left(|h_f|^2 > \frac{\nu_1}{\rho_R}\right). \end{aligned} \quad (8)$$

The final expression of the OP_{sys} can be given as in (9), shown at the bottom of the page. after substituting the CDFs (1) and (3) into (8).

D. ASYMPTOTIC OP AND DIVERSITY ORDER

The asymptotic behaviors of OP for D_f, D_n, and overall system with imperfect SIC at high SNR region is written as

$$OP_f^{\infty} = 1 - \sum_{k=0}^{m-1}\sum_{l=0}^{k} \phi_1 . \left(1 - \frac{\phi_2 \tau_1}{\rho_s}\right)\left(\frac{\tau_1}{\rho_s}\right)^l \left(1 - F_{|h_f|^2}^{\infty}\left(\frac{\nu_1}{\rho_R}\right)\right) \quad (10a)$$

$$OP_n^{\infty} = 1 - \sum_{k=0}^{m-1}\sum_{l=0}^{k} \phi_1 . \left(1 - \frac{\phi_2 \tau}{\rho_s}\right)\left(\frac{\tau}{\rho_s}\right)^l \left(1 - F_{|h_n|^2}^{\infty}\left(\frac{\nu}{\rho_R}\right)\right) \quad (10b)$$

$$\begin{aligned} OP_{sys}^{\infty} &= 1 - \sum_{k=0}^{m-1}\sum_{l=0}^{k} \phi_1 . \left(1 - \frac{\phi_2 \tau}{\rho_s}\right) . \left(\frac{\tau}{\rho_s}\right)^l \\ &\quad \times \left(1 - F_{|h_n|^2}^{\infty}\left(\frac{\nu}{\rho_R}\right)\right) . \left(1 - F_{|hf|^2}^{\infty}\left(\frac{\nu_1}{\rho_R}\right)\right), \end{aligned} \quad (10c)$$

$$\begin{aligned} OP_f &= 1 - \alpha e^{\frac{-(\beta-\delta)\tau_1}{\rho_s Q}} \sum_{k=0}^{m-1} \psi(k) \sum_{l=0}^{k} \frac{k!}{l!} \left(\frac{\tau_1}{\rho_s Q}\right)^l (\beta - \delta)^{-(k-l+1)} \\ &\quad \times \left(1 - wG_{1,2}^{1,1}\left(\frac{1}{\lambda}\left(\frac{\nu_1}{\rho_R \mu_r}\right)^{\frac{1}{r}} \middle| \begin{matrix} 1 \\ 1, 0 \end{matrix}\right) - \frac{1-w}{\Gamma(a)} G_{1,2}^{1,1}\left(\frac{1}{b^c}\left(\frac{\nu_1}{\rho_R \mu_r}\right)^{\frac{c}{r}} \middle| \begin{matrix} 1 \\ a, 0 \end{matrix}\right)\right) \end{aligned} \quad (5)$$

$$\begin{aligned} OP_n &= 1 - \alpha e^{\frac{-(\beta-\delta)\tau}{\rho_s Q}} \sum_{k=0}^{m-1} \psi(k) \sum_{l=0}^{k} \frac{k!}{l!} \left(\frac{\tau}{\rho_s Q}\right)^l \times (\beta - \delta)^{-(k-l+1)} \\ &\quad \times \left(1 - wG_{1,2}^{1,1}\left(\frac{1}{\lambda}\left(\frac{\nu}{\rho_R \mu_r}\right)^{\frac{1}{r}} \middle| \begin{matrix} 1 \\ 1, 0 \end{matrix}\right) - \frac{1-w}{\Gamma(a)} G_{1,2}^{1,1}\left(\frac{1}{b^c}\left(\frac{\nu}{\rho_R \mu_r}\right)^{\frac{c}{r}} \middle| \begin{matrix} 1 \\ a, 0 \end{matrix}\right)\right) \end{aligned} \quad (7)$$

$$\begin{aligned} OP_{sys} &= 1 - \alpha e^{\frac{-(\beta-\delta)\tau}{\rho_s Q}} \sum_{k=0}^{m-1} \psi(k) \sum_{l=0}^{k} \frac{k!}{l!} \left(\frac{\tau}{\rho_s Q}\right)^l (\beta - \delta)^{-(k-l+1)} \left(1 - \left(wG_{1,2}^{1,1}\left(\frac{1}{\lambda}\left(\frac{\nu}{\rho_R \mu_r}\right)^{\frac{1}{r}} \middle| \begin{matrix} 1 \\ 1, 0 \end{matrix}\right)\right.\right. \\ &\quad \left.\left. + \frac{1-w}{\Gamma(a)} G_{1,2}^{1,1}\left(\frac{1}{b^c}\left(\frac{\nu}{\rho_R \mu_r}\right)^{\frac{c}{r}} \middle| \begin{matrix} 1 \\ a, 0 \end{matrix}\right)\right)\right)\left(1 - \left(wG_{1,2}^{1,1}\left(\frac{1}{\lambda}\left(\frac{\nu_1}{\rho_R \mu_r}\right)^{\frac{1}{r}} \middle| \begin{matrix} 1 \\ 1, 0 \end{matrix}\right) + \frac{1-w}{\Gamma(a)} G_{1,2}^{1,1}\left(\frac{1}{b^c}\left(\frac{\nu_1}{\rho_R \mu_r}\right)^{\frac{c}{r}} \middle| \begin{matrix} 1 \\ a, 0 \end{matrix}\right)\right)\right) \end{aligned} \quad (9)$$

TABLE 1. Shadowing parameters.

Shadowing	m	α	β	δ
Frequent heavy shadowing (FHS)	1	7.8927	7.9365	0.0438
Average shadowing (AS)	5	1.1760	1.9920	0.1993
Infrequent light shadowing (ILS)	10	0.1032	3.1646	0.9174

TABLE 2. System parameters.

Symbol	Parameter	Value
S	Satellite type	Iridium LEO
h	Height of satellite	780 Km
f_s	Downlink carrier frequency	1.55 GHz
G_s	Satellite antenna gain	25 dB
G_R	Relay antenna gain	3 dB
D_s	Aperture diameter of a satellite antenna	2 m
θ_e	Satellite's pointing error angle	1°
r	Radius of the satellite's beam's coverage	200 Km
d	The distance between the relay and the beam center	0.3r m
B	Noise bandwidth	12 MHz
T	Noise temperature	290 K

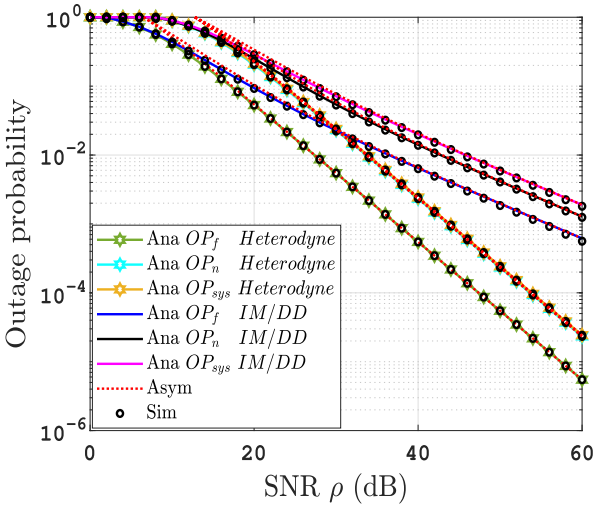

FIGURE 2. OP versus SNR for both IM/DD and heterodyne detection.

where $\phi_1 = \alpha\,\psi(k)\,\frac{k!}{l!}\,(\frac{l}{Q})^l\,(\beta-\delta)^{-(k-l+1)}$, $\phi_2 = \frac{(\beta-\delta)}{Q}$, and the asymptotic of $F^{\infty}_{|h_i|^2}$ can be given as [4], [32]

$$F^{\infty}_{|h_i|^2}(x) \approx \frac{w}{\lambda}\left(\frac{x}{\mu_r}\right)^{\frac{1}{r}} + \frac{1-w}{\Gamma(a+1)}\left(\frac{x}{b^r\mu_r}\right)^{\frac{ac}{r}}. \quad (11)$$

The diversity order (DO) is known as the slope of the asymptotic outage curves and can be calculated as $DO = -\lim_{\rho\to\infty}(\log(OP)/\log(\rho))$. After a thorough examination, one can deduce from (10) that the system diversity order (DO) is

$$DO = \min\left(l+\frac{1}{r},\, l+\frac{ac}{r}\right). \quad (12)$$

Since $ac \gg 1$ and $argmin(l) = 0$, thus DO $= \frac{1}{r}$. Therefore, we can observe that the diversity order of the system depends on the used detection techniques as confirmed in Fig. 2.

IV. RESULTS AND DISCUSSIONS

In this section, we confirm the validity of our analysis of the hybrid satellite-UOWC NOMA-based system under imperfect SIC by providing representative numerical simulations and showing the impact of various parameters on the performance of the system. The simulation results are performed over 10^6 iterations by implementing the Monte-Carlo simulation. The link between S and R is subject to Shadowed-Rician fading with variable shadowing levels where Table 1 [33] provides the channel parameters. The simulation parameters employed in this section are summarized in Table 2. We set $\eta = 0.1$ and the power allocation factors for far and near destinations to $a_f = b_f = 0.7$, $a_n = b_n = 0.3$, respectively. The target rates of the far and near destinations are $R_f = 0.5$, $R_n = 0.75$ bps/Hz, respectively. We assume that the total transmit power at satellite and relay are equal such that $\rho_s = \rho_R = \rho$. For various air bubble scenarios in thermally uniform and temperature gradient (TG)-based UOWC channels, the values of (w, λ, a, b, c) are achieved practically in [4, Tables 1, 2].

Fig. 2 shows the OPs variations against ρ for both IM/DD and heterodyne detection methods with BL= 2.4 L/min at a uniform temperature water. As can be shown, the heterodyne outperforms IM/DD detection technique in terms of OPs at both destinations and the overall system. The figure shows that the analytical curves excellently agree with the Monte-Carlo simulation, which confirms the correctness of our derivations. Furthermore, Fig. 2 shows at high SNR values the asymptotic lines of the OPs gotten by using (10). It can be observed that in the high SNR regime, the OP's asymptotic results perfectly match the analytical results, which validates the derived asymptotic equations. According to the diversity analysis, for heterodyne and IM/DD receivers, respectively, we anticipate a diversity order of 1 and 0.5, which is consistent with the findings in Fig. 2.

Fig. 3 plots the OPs versus ρ at different air BLs with a uniform temperature. It is shown from the figure that higher air BL leads to degradation of the OPs spanning the entire range of ρ attributable to a rise in water turbulence. Also, it is clear from this figure that the system performance is enhanced based on NOMA with imperfect SIC compared with the OMA scheme as the NOMA technique utilizes the spectrum more efficiently.

Fig. 4 depicts the effect of different shadowing scenarios given in Table 1 for the S-R link on the OPs for the entire range of ρ at BL = 2.4 L/min and uniform temperature. It is observed that shadowing has a considerable impact on system performance. As increased shadowing severity corresponds to worse propagation conditions, FHS results in the worst outage performance, while ILS represents the best scenario.

Fig. 5 demonstrates the OP versus the pointing error angle between the beam center and the relay with different TG. As the pointing angle increases, the outage behaviors of

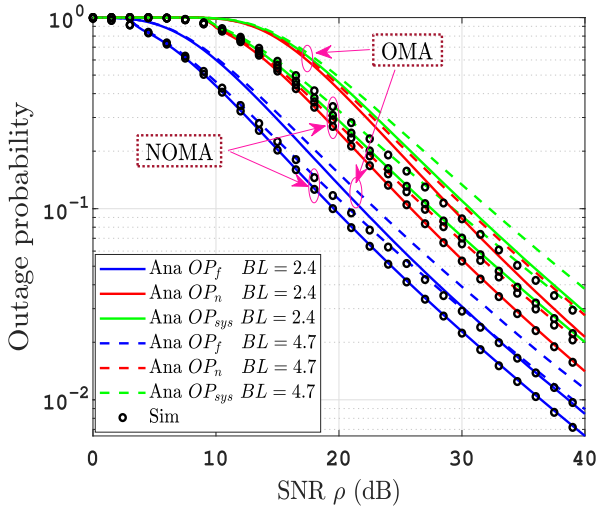

FIGURE 3. NOMA/OMA-based systems OPs versus SNR with different BLs.

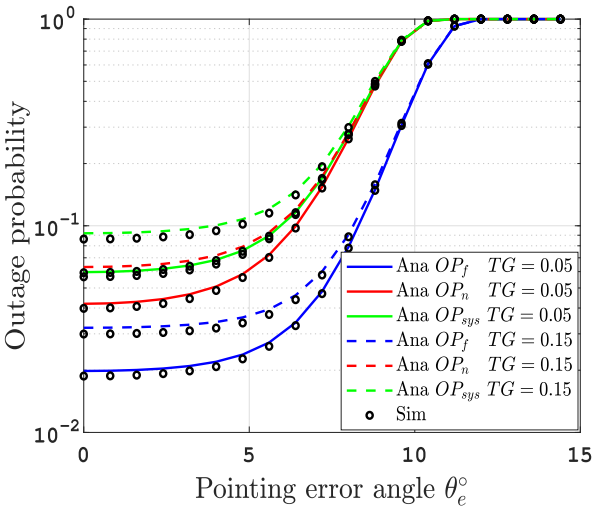

FIGURE 5. OP versus pointing error angle for different temperature gradient.

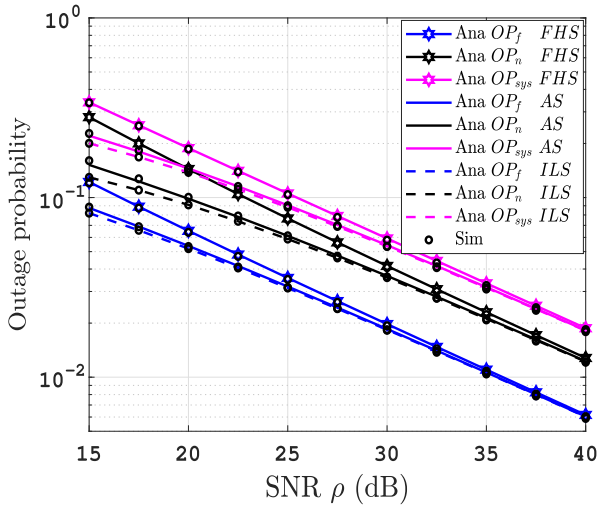

FIGURE 4. OP versus SNR with different shadowing parameters.

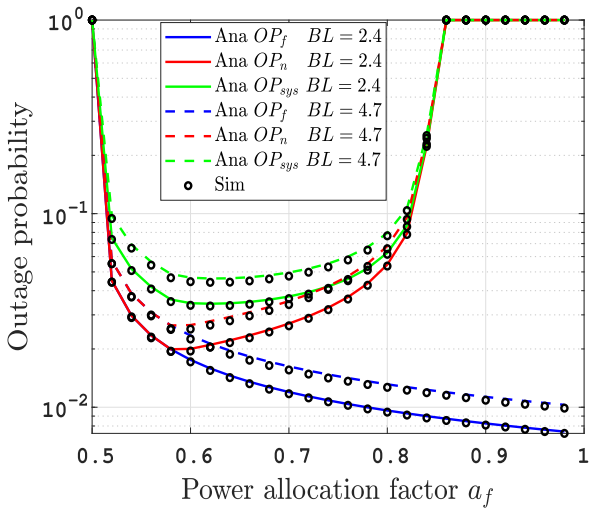

FIGURE 6. Outage probability versus power allocation factor at a uniform temperature, different air BL, and ρ= 35 dB.

both destinations and the overall system become significantly worse. For example, at $\theta_e = 12°$, the system suffers from a full outage. This is because, as the angle increases, the relay becomes closer to the edge of the received beam from the satellite. So, the satellite's beam should be adjusted to target the relay to improve system performance. Additionally, this figure demonstrates that an increase in TG from 0.05 to 0.15 °C/cm leads to a degradation in OP, for fixed BL = 2.4 L/min and $\rho = 35$ dB.

In Fig. 6, the graph for the OPs versus power allocation factor of D_f at fixed $\rho = 35$ dB is illustrated at BL = 2.4 L/min and 4.7 L/min with a uniform temperature. It is shown from the figure that with increasing power allocation factor assigned to the far destination such that $a_f = b_f$, the more power transmitted to D_f, OP_f improves while OP_n enhances in the first scene then degrades because of increase in the interference level in SINR at D_n. Additionally, it can be seen that the OPs deteriorate with a rise in BL, as the higher the BL, the higher the water turbulence.

V. CONCLUSION

In this paper, we have investigated the outage performance of the downlink NOMA-based hybrid satellite UOWC with the aid of DF relay in the case of imperfect SIC. The outage probabilities expressions of the exact and asymptotic at the two NOMA destinations and the system have been derived. We also have illustrated the effect of atmospheric conditions including shadowing, path loss, and depointing loss, as well as different underwater scenarios for salty water such as air bubbles level under uniform and temperature gradients. The results showed that an increase in water turbulence like air bubbles and temperature gradients causes degradation in outage behavior. Furthermore, an increase in atmospheric conditions like shadowing, and pointing error angle leads to a declination in outage performance. Finally, the NOMA-based outage behaviors of the proposed system with imperfect SIC outperform those of the OMA scheme.

REFERENCES

[1] V. Goutham, T. Kumar, and V. Harigovindan, "A survey on non-orthogonal multiple access with energy harvesting for underwater acoustic sensor networks," in *Proc. Int. Conf. Innov. Comput. Commun. (ICICC)*, 2021, p. 6.

[2] N. Saeed, A. Celik, T. Y. Al-Naffouri, and M.-S. Alouini, "Underwater optical wireless communications, networking, and localization: A survey," *Ad Hoc Netw.*, vol. 94, Nov. 2019, Art. no. 101935.

[3] S. Al-Zhrani et al., "Underwater optical communications: A brief overview and recent developments," *Eng. Sci.*, vol. 16, pp. 146–186, Nov. 2021.

[4] E. Zedini, H. M. Oubei, A. Kammoun, M. Hamdi, B. S. Ooi, and M.-S. Alouini, "Unified statistical channel model for turbulence-induced fading in underwater wireless optical communication systems," *IEEE Trans. Commun.*, vol. 67, no. 4, pp. 2893–2907, Apr. 2019.

[5] E. Zedini, A. Kammoun, H. Soury, M. Hamdi, and M.-S. Alouini, "Performance analysis of dual-hop underwater wireless optical communication systems over mixture exponential-generalized gamma turbulence channels," *IEEE Trans. Commun.*, vol. 68, no. 9, pp. 5718–5731, Sep. 2020.

[6] M. V. Jamali, J. A. Salehi, and F. Akhoundi, "Performance studies of underwater wireless optical communication systems with spatial diversity: MIMO scheme," *IEEE Trans. Commun.*, vol. 65, no. 3, pp. 1176–1192, Mar. 2017.

[7] K. Ye, C. Zou, and F. Yang, "Dual-hop underwater optical wireless communication system with simultaneous lightwave information and power transfer," *IEEE Photon. J.*, vol. 13, no. 6, pp. 1–7, Dec. 2021.

[8] I. S. Ansari, L. Jan, Y. Tang, L. Yang, and M. H. Zafar, "Outage and error analysis of dual-hop TAS/MRC MIMO RF-UOWC systems," *IEEE Trans. Veh. Technol.*, vol. 70, no. 10, pp. 10093–10104, Oct. 2021.

[9] S. Cioni, R. De Gaudenzi, O. D. Rio Herrero, and N. Girault, "On the satellite role in the era of 5G massive machine type communications," *IEEE Netw.*, vol. 32, no. 5, pp. 54–61, Sep./Oct. 2018.

[10] A. Gupta, N. Sharma, P. Garg, D. N. K. Jayakody, C. Y. Aleksandrovich, and J. Li, "Asymmetric satellite-underwater visible light communication system for oceanic monitoring," *IEEE Access*, vol. 7, pp. 133342–133350, 2019.

[11] V. K. Trivedi, A. Agarwal, and P. Kumar, "Performance evaluation of MC-CDMA over hybrid satellite/underwater acoustic channel," in *Proc. 10th Int. Conf. Inf. Commun. Signal Process. (ICICS)*, 2015, pp. 1–6.

[12] M. Jain, N. Sharma, A. Gupta, D. Rawal, and P. Garg, "Performance analysis of DF relaying assisted underwater visible light communication system," in *Proc. Int. Conf. Signal Process. Commun. (SPCOM)*, 2020, pp. 1–5.

[13] K. O. Odeyemi and P. A. Owolawi, "Secure hybrid satellite-UWOC cooperative relaying system under malicious unmanned aerial vehicle eavesdropper threat," *Int. J. Wireless Mobile Comput.*, vol. 21, no. 1, pp. 66–75, 2021.

[14] M. Jain, N. Sharma, A. Gupta, D. Rawal, and P. Garg, "NOMA assisted underwater visible light communication system with full-duplex cooperative relaying," *Veh. Commun.*, vol. 31, Oct. 2021, Art. no. 100359.

[15] K. W. S. Palitharathna, H. A. Suraweera, R. I. Godaliyadda, V. R. Herath, and J. S. Thompson, "Average rate analysis of cooperative NOMA aided underwater optical wireless systems," *IEEE Open J. Commun. Soc.*, vol. 2, pp. 2292–2310, 2021.

[16] X. Li, Z. Xie, Z. Chu, V. G. Menon, S. Mumtaz, and J. Zhang, "Exploiting benefits of IRS in wireless powered NOMA networks," *IEEE Trans. Green Commun. Netw.*, vol. 6, no. 1, pp. 175–186, Mar. 2022.

[17] A. Samir, M. Elsayed, A. A. A. El-Banna, K. Wu, and B. M. ElHalawany, "Performance of NOMA-based dual-hop hybrid powerline-wireless communication systems," *IEEE Trans. Veh. Technol.*, vol. 71, no. 6, pp. 6548–6558, Jun. 2022.

[18] X. Li, J. Li, Y. Liu, Z. Ding, and A. Nallanathan, "Residual transceiver hardware impairments on cooperative NOMA networks," *IEEE Trans. Wireless Commun.*, vol. 19, no. 1, pp. 680–695, Jan. 2020.

[19] B. M. ElHalawany, F. Jameel, D. B. da Costa, U. S. Dias, and K. Wu, "Performance analysis of downlink NOMA systems over κ-μ shadowed fading channels," *IEEE Trans. Veh. Technol.*, vol. 69, no. 1, pp. 1046–1050, Jan. 2020.

[20] C. Gamal et al., "Performance of hybrid satellite-UAV NOMA systems," in *Proc. IEEE Int. Conf. Commun. (ICC)*, 2022, pp. 189–194.

[21] W. U. Khan, X. Li, A. Ihsan, Z. Ali, B. M. Elhalawany, and G. A. S. Sidhu, "Energy efficiency maximization for beyond 5G NOMA-enabled heterogeneous networks," *Peer-to-Peer Netw. Appl.*, vol. 14, no. 5, pp. 3250–3264, 2021.

[22] B. M. ElHalawany, A. A. A. El-Banna, Q.-V. Pham, K. Wu, and E. M. Mohamed, "Spectrum sharing in cognitive-radio-inspired NOMA systems under imperfect SIC and cochannel interference," *IEEE Syst. J.*, vol. 16, no. 1, pp. 1540–1547, Mar. 2022.

[23] X. Yue, Z. Qin, Y. Liu, S. Kang, and Y. Chen, "A unified framework for non-orthogonal multiple access," *IEEE Trans. Commun.*, vol. 66, no. 11, pp. 5346–5359, Nov. 2018.

[24] C. Brekke and A. H. S. Solberg, "Oil spill detection by satellite remote sensing," *Remote Sens. Environ.*, vol. 95, no. 1, pp. 1–13, 2005.

[25] M. Mityagina and O. Lavrova, "Satellite survey of offshore oil seep sites in the caspian sea," *Remote Sens.*, vol. 14, no. 3, p. 525, 2022.

[26] D. Zwillinger and A. Jeffrey, *Table of Integrals, Series, and Products*. Amsterdam, The Netherlands: Elsevier, 2007.

[27] J. Arnau, D. Christopoulos, S. Chatzinotas, C. Mosquera, and B. Ottersten, "Performance of the multibeam satellite return link with correlated rain attenuation," *IEEE Trans. Wireless Commun.*, vol. 13, no. 11, pp. 6286–6299, Nov. 2014.

[28] G. Maral, M. Bousquet, and Z. Sun, *Satellite Communications Systems: Systems, Techniques and Technology*. Hoboken, NJ, USA: Wiley, 2020.

[29] A. Samir, M. Elsayed, A. A. A. El-Banna, I. S. Ansari, K. Rabie, and B. M. ElHalawany, "Performance analysis of dual-hop hybrid RF-UOWC NOMA systems," *Sensors*, vol. 22, no. 12, p. 4521, 2022.

[30] N.-L. Nguyen, H.-N. Nguyen, A.-T. Le, D.-T. Do, and M. Voznak, "On performance analysis of NOMA-aided hybrid satellite terrestrial relay with application in small-cell network," *IEEE Access*, vol. 8, pp. 188526–188537, 2020.

[31] B. M. ElHalawany, A. Samir, M. Elsayed, W. U. Khan, K. Wu, and E. M. Mohamed, "Outage and capacity analysis of NOMA systems over dual-hop mixed powerline-wireless channels," *ICT Exp.*, to be published.

[32] M. Elsayed, A. Samir, A. A. A. El-Banna, W. U. Khan, S. Chatzinotas, and B. M. ElHalawany, "Mixed RIS-relay NOMA-based RF-UOWC systems," in *Proc. IEEE 95th VTC-Spring*, 2022, pp. 1–6.

[33] H. Shuai, K. Guo, K. An, and S. Zhu, "NOMA-based integrated satellite terrestrial networks with relay selection and imperfect SIC," *IEEE Access*, vol. 9, pp. 111346–111357, 2021.

CHRISTINA GAMAL (Student Member, IEEE) received the B.Sc. degree in electronics and communication engineering and the M.Sc. degree in communication engineering from the Faculty of Engineering at Shoubra, Benha University, Egypt, in 2013 and 2019, respectively. She is currently pursuing the Ph.D. degree in communication engineering. She is currently an Assistant Lecturer with the Faculty of Engineering at Shoubra, Benha University. Her current research interests include satellite, non-orthogonal multiple access, and unmanned aerial vehicles.

MOHAMED ELSAYED (Student Member, IEEE) received the M.Sc. and Ph.D. degrees in electronics engineering from the Faculty of Engineering at Shoubra, Benha University, Egypt, in 2017 and in 2022, respectively, where he is currently a Lecturer. He has authored or coauthored of 10 high quality research papers in international leading journals and conferences. His research interests include performance analysis, and optimization in wireless networks, NOMA, backscatter communication, hybrid communication system, and underwater and satellite communication networks.

AHMED SAMIR (Student Member, IEEE) received the M.Sc. and Ph.D. degrees in electronics engineering from the Faculty of Engineering at Shoubra, Benha University, Egypt, in 2017 and 2022, respectively, where he is currently a Lecturer. He has authored or coauthored of 10 high quality research papers in international leading journals and conferences. His research interests include performance analysis, and optimization in wireless networks, NOMA, backscatter communication, hybrid communication system, and underwater and satellite communication networks.

HEBA A. TAGELDIEN received the B.Sc., M.Sc., and Ph.D. degrees from the Faculty of Engineering at Shoubra, Benha University, Egypt, in 2007, 2013, and 2017, respectively, where she is currently an Associate Professor with the Electrical Engineering Department. Her research interests include Networks, CRN, SDN, wireless communication, IOT machine learning, and satellite communication.

SYMEON CHATZINOTAS (Senior Member, IEEE) is a Full Professor and the Head of the SIGCOM Research Group at SnT, University of Luxembourg. In the past, he has been a Visiting Professor with the University of Parma, Italy, and was involved in numerous research and development projects for NCSR Demokritos, CERTH Hellas, and CCSR with the University of Surrey. He is coordinating the research activities on communications and networking across a group of 80 researchers, acting as a PI for more than 40 projects and main representative for 3GPP, ETSI, and DVB. He has coauthored more than 700 technical papers in refereed international journals, conferences, and scientific books. He was the co-recipient of the 2014 IEEE Distinguished Contributions to Satellite Communications Award and the Best Paper Awards at WCNC, 5GWF, EURASIP JWCN, CROWNCOM, and ICSSC. He is currently serving in the editorial board of the IEEE TRANSACTIONS ON COMMUNICATIONS, IEEE OPEN JOURNAL OF VEHICULAR TECHNOLOGY, and the *International Journal of Satellite Communications and Networking*.

MOSTAFA M. FOUDA (Senior Member, IEEE) received the B.S. degree (as the valedictorian) and the M.S. degree in electrical engineering from Benha University, Egypt, in 2002 and 2007, respectively, and the Ph.D. degree in information sciences from Tohoku University, Japan, in 2011. He is currently an Assistant Professor with the Department of Electrical and Computer Engineering, Idaho State University, Pocatello, ID, USA. He also holds the position of a Full Professor with Benha University. He was an Assistant Professor with Tohoku University and a Postdoctoral Research Associate with Tennessee Technological University, Cookeville, TN, USA. He has coauthored more than 130 technical publications. His current research focuses on cybersecurity, communication networks, signal processing, wireless mobile communications, smart healthcare, smart grids, AI, and IoT. He is currently serving on the editorial board of IEEE TRANSACTIONS ON VEHICULAR TECHNOLOGY and IEEE ACCESS. He has received several research grants, including NSF Japan-U.S. Network Opportunity 3. He has guest-edited a number of special issues covering various emerging topics in communications, networking, and health analytics.

BASEM M.ELHALAWANY (Senior Member, IEEE) received the master's degree from Benha University, Banha, Egypt, in 2011, and the Ph.D. degree from the Egypt-Japan University of Science and Technology, New Borg El Arab, Egypt, in 2014. He was a Research Fellow with Smart Sensing and Mobile Computing Laboratory, Shenzhen University, Shenzhen, China, and EJUST Center, Kyushu University, Fukuoka, Japan. He also holds the position of an Associate Professor with the Faculty of Engineering at Shoubra, Benha University. He has authored or coauthored more than 60 high quality research papers in international leading journals and primer conferences. His research interests include performance analysis, resource management, and optimization in wireless networks, NOMA, underwater and satellite communication networks, and machine learning applications in communication. He is an Associate Editor of *Alexandria Engineering Journal*.